Journal of Aeronautics, Astronautics and Aviation, Vol. 52, No. 4, pp. 403 – 416 (2020)
DOI: 10.6125/JoAAA.202012_52(4).0X

Measurement-Domain Cooperative Navigation for Multi-UAV Systems Augmented by Relative Positions *

Xiyu Liu, Xingqun Zhan **, Shizhuang Wang, and Yawei Zhai

School of Aeronautics and Astronautics, Shanghai Jiao Tong University
No.800, Dongchuan Rd., Minhang District, Shanghai 200240, China.

ABSTRACT

This paper proposes a novel cooperative navigation scheme to support multiple Unmanned Aerial Vehicle (UAV) formation flight. Comparing to standalone Global Navigation Satellite System (GNSS), the new approach takes advantage of inner communication capability among UAVs to achieve navigation information fusion. As a result, the navigation accuracy, robustness and continuity can be improved. This is of particular significance in urban environments, because the user receivers are subject to high multipath, non-line-of-sight signal reception and signal blockage. With the aid of relative sensing technologies, all the GNSS observations are firstly combined to estimate the position of a designated point (defined as virtual centroid). Then, the positions of each individual UAV are derived by fusing the position estimate of virtual centroid and the known relative positions. This method is implemented, validated, and analyzed through a series of simulations, and the results suggest significant accuracy improvement as compared to standalone GNSS approaches. Moreover, sensitivity analyses are carried out to address the impact of environmental changes on navigation performance.

Keywords: Cooperative Navigation, Global Navigation Satellite System (GNSS), Unmanned Aerial Vehicle (UAV), Formation Flight, Relative Navigation

I. INTRODUCTION

Multiple Unmanned Aerial Vehicle (UAV) swarming technology has received a lot of attention over the past decades. The prospect is seen in both civil and military fields, e.g. commercial UAV show, Simultaneous Localization And Mapping (SLAM), patrol mission, swarm attack and trajectory planning [1][2]. Among all navigational techniques, knowing the exact position of each vehicle is the bedrock to perform an outdoor UAV swarm.

Global Navigation Satellite System (GNSS) [3] is a basic and indispensable technique for a UAV swarm, yet the sensitivity to GNSS jamming signals makes it vulnerable in urban environments, owing to multipath, GNSS blockages and reception of non-Line-of-Sight (NLOS) signals. To mitigate this issue, groups of vehicles work together and share information, which is called cooperative navigation. In addition, relative navigation is proposed, which achieves high accurate navigation using Ultra-Wide Band (UWB), vision, Real-Time Kinematic (RTK), Light Detection and Ranging (LiDAR), Dedicated Short Range Communication (DSRC)[4][5][6], etc.

Cooperative navigation is an efficient technique for Multi-UAV formation flight that vehicles in the network cooperate to estimate their positions. In comparison, traditional navigation methods only rely on the GNSS information of single UAV. Thanks to various approaches of inner-UAV data transmission, such as Wi-Fi, Bluetooth, Zigbee, cellular network, etc., UAVs can share both absolute and relative observations in a swarm system, which increases redundant information and thus improves the efficiency and robustness of the whole system.

* Manuscript received, June 29, 2020, final revision, September 18, 2020
** To whom correspondence should be addressed, E-mail: xqzhan@sjtu.edu.cn

In the literature, multi-UAV cooperative navigation is realized with various approaches. An approach proposed by N. Merlinge et al. was to share absolute navigation results across UAVs to realize cooperative IMU hybridization [7]. T. M. Nguyen et al. proposed a cooperative estimation-control scheme where UWB and optical flow sensors are employed along with IMU and magnetometers to realize cooperative relative navigation [8]. Y. Qu et al. utilized relative angles to reference UAVs to achieve fault-tolerant positioning in a cooperative flight [9].

Several other studies provide solutions for cooperative navigation in urban environments. A cooperative multi-UAV algorithm proposed by A. R. Vetrella et al. aimed at enhancing the navigation performance of a chief vehicle with differential GPS (DGPS), camera, IMU and magnetic sensors [10]. In this method, the deputy vehicles were required to be placed in a fixed known location and acted as anchor nodes. A cooperative two-vehicle system was proposed by V. O. Sivaneri et al., where the UAV was assisted by a cooperative Unmanned Ground Vehicle (UGV) through the combination of GNSS observations and peer-to-peer radio ranging measurements [11][12]. However, a swarm of more than two vehicles has not been validated in this strategy. H. Ko et al. proposed a cooperative positioning method in urban vehicular networks which broadcasts vehicle's absolute position and gets V2V range measurements with UWB [13]. It solves a 2D cooperative positioning problem and has not been proved on UAV platforms.

As far as we know, there is no study that guarantees high accuracy absolute navigation for a multi-UAV swarm without the help of anchor nodes. Anchor nodes can either be stationary GNSS receivers with known positions or moving vehicles equipped with high-end navigation devices. The former requires additional costs on the deployment of ground stations as part of the swarm, and the latter may vitiate the navigation performance of the swarm when the anchor node itself crosses urban environments. Thus, an anchor-free swarming technology is worth further research.

This paper focuses on resolving anchor-free multi-UAV cooperative navigation problems. A novel approach is proposed to make full use of GNSS observations and relative measurements from all UAVs to achieve high robustness in urban environments. It aims at enhancing the accuracy of absolute navigation of the swarm. Among all the state estimation algorithms, we adopt Weighted Least-Squares (WLS) to provide position solution due to its low complexity and direct data processing. In the practice of urban cooperative navigation, signal attenuation and communication delay should be considered. However, it is beyond the scope and will not be discussed in this paper. The proposed approach helps reduce the uncertainty of absolute navigation with complementary GNSS observations. Additionally, we compare the efficiency of cooperative navigation and standalone GNSS navigation in urban environments.

The paper is organized as follows. In Section 2, we deliver a description of the concept and model used in the approach. Our algorithm along with sensitivity analysis is presented in Section 3. Section 4 gives both environment settings and simulation results. Conclusions are presented in Section 5.

II. PROBLEM FORMULATION AND SYSTEM MODELLING

This section elucidates the problem to be solved and presents all the measurement models and the corresponding error models which are involved in our approach. Covariance matrices are introduced to describe the error of the measurements, which also makes a foundation for the sensitivity analysis. An innovative measurement transfer method is developed to process the input data before position calculation.

2.1 Problem Statement

Multi-UAV formation flight has great market potential. However, swarms may face challenges when operating in urban environments. Some UAVs may encounter multipath, NLOS signal reception and signal loss, which brings about huge navigation error in standalone GNSS navigation. Due to the increasing number of base stations in urban areas, absolute navigation can be largely improved with differential correction, whereas multipath and receiver related error remains. In this respect, cooperative navigation can address the issue with inner-UAV communication technology and relative navigation system.

In GNSS blocked environments, relative measurements can be a good aid for navigation because they are less susceptible to multipath and blockages compared with GNSS measurements [14]. Those relative measurements can be obtained through various sensors such as UWB, vision, RTK, LiDAR, and DSRC, etc.

For instance, UWB technology is combined with relative positions between one and neighboring vehicles in Vehicular Ad-Hoc Networks (VANETs) to improve relative navigation accuracy [15]. Range rate estimated by DSRC based on Doppler shift can be integrated with GNSS observations, which reduces 2D navigation error with stable precision [16].

Relative measurements can be classified as distance estimates, angle estimates and displacement estimates. Relative position data can be easily acquired by merging the foregoing relative measurements with state estimation algorithms such as Least Squares, Kalman Filter, factor graph and so on [7][17][18].

By fusing additional measurements, cooperative navigation improves the navigation accuracy of the UAV swarm.

2.2 Measurement Models

The measurements of our cooperative navigation algorithm are composed of GNSS data and relative measurements.

GNSS data includes observation data generated from a receiver and information of satellite orbits that comes from ephemeris data. In this paper, we focus on processing pseudorange observations rather than carrier-phase

measurements because the problem of cycle slips remains challenging in calculating the phase ambiguity. The pseudorange observation of receiver r and satellite k is presented as:

$$\rho_r^k = d_r^k + c(\delta t_r - \delta t^k) + I_r^k + T_r^k + \varepsilon_r^k \quad (1)$$

where:
c is the speed of light;
δt^k and δt_r are the clock offset in satellite and receiver, respectively;
I and T are the ionosphere and troposphere error due to signal propagation separately;
ε is the error caused by multipath and thermal noise in the receiver;
d denotes the true geometrical distance, for example, d_r^k can be calculated according to the kth satellite coordinates (x^k, y^k, z^k) and the receiver coordinates (x_r, y_r, z_r) by:

$$d_r^k = \sqrt{(x^k - x_r)^2 + (y^k - y_r)^2 + (z^k - z_r)^2} \quad (2)$$

To eliminate the effect of ionospheric delay, linear combination is applied on pseudorange measurements with the help of common dual-frequency receivers. This step is called ionosphere-free combination [19].

It is assumed that all the measurement residuals follow independent zero-mean Gaussian distribution. The measurement covariance matrix for GNSS standalone single point navigation is defined by:

$$\boldsymbol{C}(i,i) = \sigma_{URE,i}^2 + \sigma_{tropo,i}^2 + \sigma_{user,i}^2 \quad (3)$$

where $\sigma_{URE,i}$ is the standard deviation of the clock and ephemeris error of satellite i; $\sigma_{tropo,i}$ is the standard deviation of tropospheric delay; $\sigma_{user,i}$ represents the receiver-related error prediction.

The error models for the terms mentioned are established as follows [20]:

$$\sigma_{URE,i} = 1 \quad (4)$$

$$\sigma_{tropo,i}(\theta) = 0.12\frac{1.001}{\sqrt{0.002001 + \sin^2\left(\frac{\pi\theta}{180}\right)}} \quad (5)$$

$$\sigma_{MP,i}(\theta) = 0.13 + 0.53\exp(-\theta/10) \quad (6)$$

$$\sigma_{Noise,i}(\theta) = 0.15 + 0.43\exp(-\theta/6.9) \quad (7)$$

$$\sigma_{user,i} = \sqrt{\frac{f_{L1}^4 + f_{L2}^4}{(f_{L1}^2 - f_{L2}^2)^2}} \cdot \sqrt{\sigma_{MP,i}^2 + \sigma_{Noise,i}^2} \quad (8)$$

where $\sigma_{MP,i}$ and $\sigma_{Noise,i}$ are respectively the standard deviation of multipath error and the error related to thermal noise in the GNSS receiver; θ is the elevation angle in degrees. Ionospheric delay is not considered when applying ionosphere-free combination to the GNSS measurements. The calculation follows International System of Units (SI) and is presented in meters.

In order to validate the algorithm proposed in this paper, we assume that relative observations have already been fused into relative positions. The relative position measurement can be expressed as:

$$\boldsymbol{x} = \boldsymbol{l} + \boldsymbol{\epsilon} \quad (9)$$

where:
$\boldsymbol{l}$ is the actual relative position between two UAVs;
$\boldsymbol{\epsilon}$ is the relative ranging error in three dimensions. In each dimension, the error can be described as a Gaussian noise $N(0, \sigma_d^2)$, where σ_d^2 incorporates the diagonal element of the covariance matrix for fused relative position observations $\boldsymbol{C}_d$. It is assumed that relative positions are imposed by the same standard deviation of error in each dimension.

2.3 Navigation Information Fusion based on Measurement Transfer

Inspired by the differential navigation methods in GNSS relative navigation, GNSS measurements can be transferred to a certain point based on the knowledge of relative positions. The results are termed equivalent GNSS measurements. In fact, pseudorange transfer can be seen as the reverse of Differential GNSS (DGNSS) navigation. Firstly, the relative navigation data as well as GNSS measurements are collected. Then the GNSS measurements can be transferred to the position of a certain point by means of single or double differenced transfer method.

Referring to the single differenced pseudorange equation for receiver *r*, designated point *b* and satellite *k*, the transfer result ρ_b^k can be calculated by:

$$\rho_b^k = \rho_r^k + \rho_{rb}^k = \rho_r^k + d_{rb}^k + c\delta t_{rb} + \varepsilon_{rb}^k \quad (10)$$

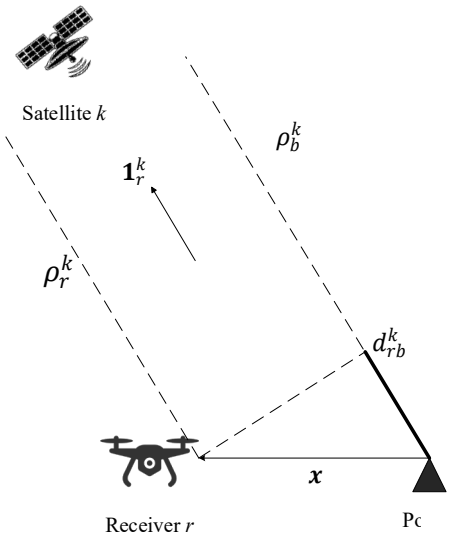

Figure 1 Equivalent GNSS measurement for point b in SDT method

where:

δt_{rb} represents the difference of the clock bias, i.e. relative clock bias, between receiver r and point b;

ε_{rb}^k indicates the difference of error between receiver r and point b;

d_{rb}^k is the vector projection which is given by:

$$d_{rb}^k = \mathbf{1}_r^k \cdot \boldsymbol{x} \tag{11}$$

where:

$\mathbf{1}_r^k$ is the Line-of-Sight (LOS) unit vector which originates from receiver and points toward satellite k;

$\boldsymbol{x}$ which is called baseline, is the relative position between receiver and the point.

In Equation 11, it is indispensable to provide the relative clock bias in order to perform the Single Differenced Transfer (SDT) method. To obtain this parameter, the reader may refer to between-receiver DGNSS positioning, which requires at least $3 + N_{const}$ satellites. Here N_{const} represents the number of constellations. If another receiver is designated as point b, follow the DGNSS navigation method to calculate the relative clock bias, otherwise assume the value equals to 0.

Meanwhile, the Double Differenced Transfer (DDT) method is defined as:

$$\rho_b^k = \rho_r^k + \rho_b^j - \rho_r^j + \rho_{rb}^{jk} = \rho_r^k + \rho_{rb}^j + d_{rb}^{jk} + \varepsilon_{rb}^{jk} \tag{12}$$

where j is elected as the reference satellite.

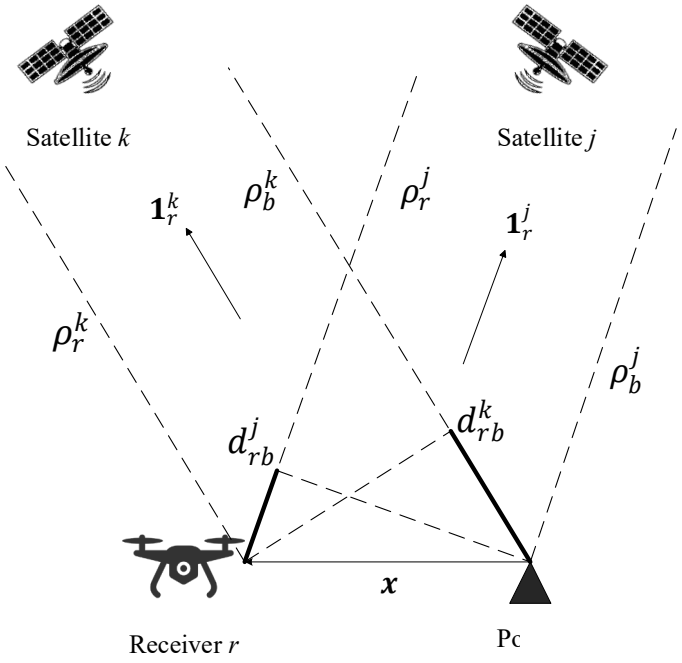

Figure 2 Equivalent GNSS measurement for point b in DDT method

Accordingly, the difference of vector projection can be derived by:

$$d_{rb}^{jk} = (\mathbf{1}_r^k - \mathbf{1}_r^j) \cdot \boldsymbol{x} \tag{13}$$

In Figure 2, the variable d_{rb}^{jk} is expressed as the difference of d_{rb}^{j} and d_{rb}^{k}.

Comparing to SDT, relative clock bias is absent from the DDT method. Moreover, a pivot satellite, usually the one with highest elevation angle, must be selected as the reference satellite before operating the double differenced method. The GNSS observations are transferred in the application of double differenced method based on the assumption that the pseudorange between the pivot satellite and point b is available. In this case, only receivers can be labelled as point b, which generate first-hand pseudorange resource. In other words, SDT method places more stringent demands on the number of satellites, whereas DDT only asks for one visible satellite.

III. METHODOLOGY AND ANALYSIS

Based on the models established in Section Ⅱ, this section introduces the procedures of processing the raw navigation data in Figure 3. WLS is selected to estimate the absolute position of virtual centroid. The effectiveness of this approach is proved by a sensitivity analysis and then validated by the numerical results in the next section.

3.1 The Selection of Virtual Centroid

To realize the cooperative navigation, we propose an innovative method named measurement transfer to virtual centroid. The position of virtual centroid is acquired based on the relative position of the nodes in the network.

A fixed point can be chosen as the virtual centroid. Note that UAVs select the virtual centroid separately. In this paper, each UAV designates itself as virtual centroid. To be concise, the variables, vectors and matrices related to virtual centroid will be denoted by an asterisk as a superscript, e.g. ρ^*, to replace ρ_b in Section 2.

The overall logical architecture of the proposed cooperative navigation algorithm is presented in Figure 3 where input data include: GNSS observations from all UAVs in the swarm and fused relative position measurements. The processing of information fusion follows either SDT or DDT method to obtain equivalent GNSS measurements for virtual centroid. With the handling of absolute measurements, the position of virtual centroid can be calculated. Finally, all the UAVs get located based on the knowledge of relative position between virtual centroid and themselves.

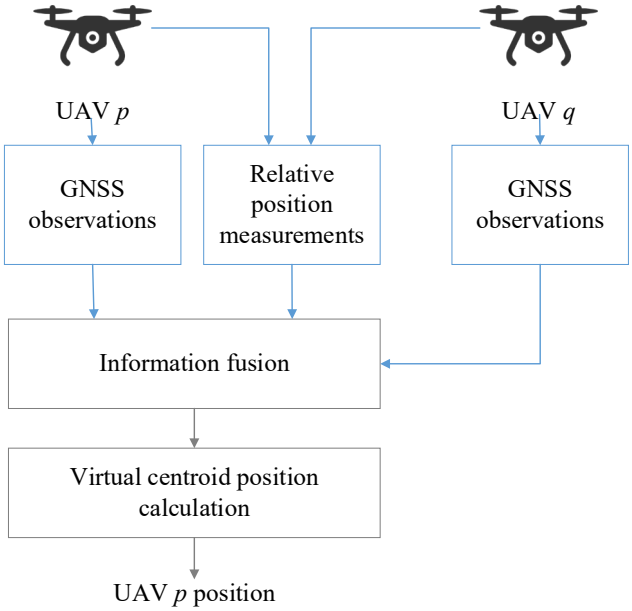

Figure 3 The proposed cooperative navigation algorithm based on virtual centroid

In traditional cooperative navigation methods, one or more UAVs are equipped with high-end sensors and thus are called masters. Their duty is to assist those suffer from poor position estimates, called slaves, by broadcasting their absolute positions to the slaves. Then slaves fuse the relative positions between masters and themselves and the received absolute positions of masters to calculate their own positions. As a result, the GNSS observations from slaves are wasted and make no contributions to positioning results. In the cooperative navigation approach proposed in this paper, observations are fully exploited to lower the positioning error in terms of multipath and receiver noise.

3.2 Weighted Least-Squares Estimation

We adopt WLS method [21] to estimate the position of virtual centroid in the approach.

For a UAV swarm, it is assumed that in one epoch altogether m pseudorange observations are updated and

then fused into m equivalent pseudorange measurements. Here $m \leq N_s \times N_v$, where N_s and N_v respectively denote the number of satellites and UAVs. The equation for WLS is illustrated as:

$$\begin{bmatrix} -\left(\mathbf{1}^{(1)}\right)^T & 1 \\ -\left(\mathbf{1}^{(2)}\right)^T & 1 \\ \vdots & \vdots \\ -\left(\mathbf{1}^{(m)}\right)^T & 1 \end{bmatrix} \cdot \begin{bmatrix} \Delta x \\ \Delta y \\ \Delta z \\ \Delta\delta t^* \end{bmatrix} = \begin{bmatrix} \rho^{*(1)} - d^{*(1)} - \delta t^* \\ \rho^{*(2)} - d^{*(2)} - \delta t^* \\ \vdots \\ \rho^{*(m)} - d^{*(m)} - \delta t^* \end{bmatrix} \quad (14)$$
$$\overset{\Delta}{\Leftrightarrow} \boldsymbol{G} \cdot \Delta\boldsymbol{p} = \boldsymbol{a}$$

where:

$\mathbf{1}$ is the LOS unit vector which points toward a certain satellite. The LOS unit vectors are shared among the swarm because the distance between UAVs is relatively short compared to the one from a UAV to a satellite.

x, y and z represents the position of virtual centroid in ECEF coordinates, which then simplified as $\boldsymbol{p}$ together with the clock bias of virtual centroid δt^*;

Δx, Δy and Δz are the update of position in three directions respectively;

ρ^* is the equivalent GNSS observation at virtual centroid, which is acquired by using SDT or DDT method;

d^* is the calculated geometrical distance between a certain satellite and virtual centroid, which generates from each iteration;

$\boldsymbol{G}$ is a Jacobian matrix which is usually termed geometry matrix.

The solution for the above equation is

$$\Delta\boldsymbol{p} = (\boldsymbol{G}^{\mathrm{T}}\boldsymbol{W}\boldsymbol{G})^{-1}\boldsymbol{G}^{\mathrm{T}}\boldsymbol{W}\boldsymbol{a} \quad (15)$$

The iteration starts with an initial vector of all zeros $\boldsymbol{p}$, the length of which equals to $3 + N_{const}$.

The weight matrix is established as:

$$\boldsymbol{W} = \boldsymbol{C}^{-1} \quad (16)$$

where $\boldsymbol{C}$ represents the covariance matrix of the measurement noise. This equation is suitable for both GNSS standalone navigation and the cooperative navigation method we propose.

After implementing WLS to estimate the location of the virtual centroid, each UAV fuses the positioning solution of the virtual centroid with the relative position between itself and the virtual centroid so as to estimate the position of itself.

3.3 Uncertainty Estimation

In order to numerically assess the positioning performance of the two approaches, we use covariance matrices to perform sensitivity analyses. Covariance matrices are derived based on the understanding of linear transformation of matrices.

We can derive the covariance matrix of positioning error for standalone GNSS navigation

$$\boldsymbol{H} = (\boldsymbol{G}^{\mathrm{T}}\boldsymbol{C}^{-1}\boldsymbol{G})^{-1} \quad (17)$$

which is compatible with the proposed cooperative navigation approach. However, different observation covariance matrices should be built for the two navigation methods.

Due to the import of relative measurement error, the observation covariance matrix of virtual centroid $\boldsymbol{C}^*$ is more complicated for cooperative navigation. Consider a covariance for the error of two equivalent GNSS measurements. The first comes from receiver p and targets the jth satellite while the second is transferred from receiver q and focuses on satellite k. To simplify the notation for an error variable, a top tilde is adopted, e.g. $\tilde{\rho}$. The covariance can be expressed as:

$$\mathrm{cov}\left(\tilde{\rho}_p^{*j}, \tilde{\rho}_q^{*k}\right) = \begin{cases} \sigma_{URE,j}^2 + \sigma_{tropo,j}^2 + \sigma_{user,j}^2 + \sigma_d^2, & j = k, p = q \\ \sigma_{URE,j}^2 + \sigma_{tropo,j}^2, & j = k, p \neq q \\ \sigma_d^2 \cdot \cos\left(\theta_{jk}\right), & j \neq k, p = q \\ 0, & j \neq k, p \neq q \end{cases} \quad (18)$$

where θ_{jk} is the angle between Line-of-Sight (LOS) satellite vector $\mathbf{1}^j$ and $\mathbf{1}^k$.

Each element in $\boldsymbol{C}^*$ is calculated according to Eq. 18. A detailed proof is provided in Appendix. Then the calculation of the covariance matrix for positioning error of virtual centroid $\boldsymbol{H}^*$ follows Eq. 17.

In order to get the theoretical standard deviation of the positioning error for each UAV, the covariance matrices should be transferred from virtual centroid to certain UAVs. During this step, relative measurement error is once again introduced. The error propagation model for the position of UAV p is established as:

$$\boldsymbol{H}_p = \boldsymbol{H}^* + \left(1 + 2 \cdot \boldsymbol{S}^* \cdot \boldsymbol{E}_p\right) \cdot \boldsymbol{C}_d \quad (19)$$

where:

$\boldsymbol{C}_d$ presents relative position covariance matrix;

$\boldsymbol{S}$ is defined by geometry matrix $\boldsymbol{G}$ and weight $\boldsymbol{W}$

$$\boldsymbol{S} = (\boldsymbol{G}^{\mathrm{T}}\boldsymbol{W}\boldsymbol{G})^{-1}\boldsymbol{G}^{\mathrm{T}}\boldsymbol{W} \quad (20)$$

$\boldsymbol{E}_p$ consists of LOS vectors which are partitioned into

$$\boldsymbol{E}_p = \begin{bmatrix} \boldsymbol{E}_p^1 \\ \boldsymbol{E}_p^2 \\ \vdots \\ \boldsymbol{E}_p^{N_{ts}} \end{bmatrix} \quad (21)$$

A partition matrix for jth satellite is arranged as

$$\boldsymbol{E}_p^j(i) = \begin{cases} \mathbf{1}^j, & i = p \\ \mathbf{0}_{1\times 3}, & i \neq p \end{cases} \quad (22)$$

Here N_{ts} represents the total number of satellites that are visible to the whole swarm rather than the one for a particular UAV.

To evaluate the authenticity of the positioning covariance matrices derived from the variance of GNSS

observations and relative measurements, we define SIG as the theoretical standard deviation for the positioning error:

$$\begin{bmatrix}\tilde{\sigma}_e\\ \tilde{\sigma}_n\\ \tilde{\sigma}_u\end{bmatrix} = \begin{bmatrix}\sqrt{\boldsymbol{H}(1,1)}\\ \sqrt{\boldsymbol{H}(2,2)}\\ \sqrt{\boldsymbol{H}(3,3)}\end{bmatrix} \tag{23}$$

which is expected to be consistent with statistical standard deviation for the positioning error.

The uncertainty level of cooperative navigation with the provision of high-quality relative measurements is proved lower than the one of GNSS standalone navigation. Let us consider a rather ideal case that all UAVs are exposed in the open sky and have access to differential correction, meanwhile the relative positioning error equals to zero. The relationship between $\boldsymbol{H}$ and $\boldsymbol{H}^*$ can be expressed as

$$\boldsymbol{H}^* = \frac{\boldsymbol{H}}{N_v} \tag{24}$$

However, it is difficult to compare $\boldsymbol{H}$ and $\boldsymbol{H}^*$ when we take into consideration all the environmental parameters, i.e. N_s, N_v and $\boldsymbol{C}_d$. We will further analyze the uncertainty levels in the next section with simulation results.

IV. RESULTS AND DISCUSSION

This section will discuss the simulation results and compare the positioning performances based on different approaches. We will first present the simulation settings and then display the test results on positioning accuracy. Finally, we will carry out sensitivity analyses of external environments based on simulation results.

4.1 Simulation Settings and Scenarios

To validate the proposed approach, a numerical simulation was performed under the initial circumstances that 5 UAVs form the swarm among which one vehicle is affected by GNSS blockage. As in Figure 4, dots are used to represent UAVs in a fixed formation. The blue ones are those in the open sky while the red one is susceptible to urban street canyons. The standard deviation of relative position error reaches [0.5, 0.5, 0.5] m in ENU coordinates. The simulation acts as a post-processing procedure and based on the assumption of unconstrained bandwidth and nonglossy communication.

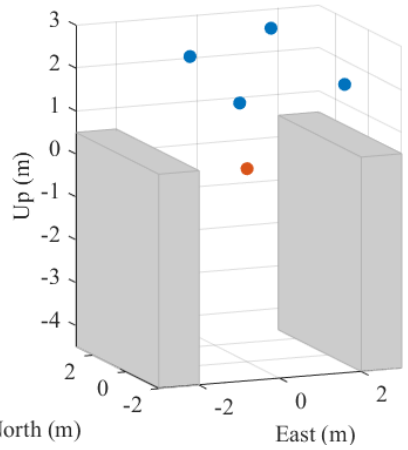

Figure 4 Default UAV formation geometry

Due to the fact that this approach aims to enhance the positioning performance especially for the UAVs in GNSS blocked environments, an elevation mask is applied to simulate urban settings (See Figure 5).

The elevation mask for the urban environment is modelled as [22]:

$$\theta_m(\varphi_m) = |\mathrm{atan}(h/d \cdot \sin(\varphi_m))| \tag{25}$$

where θ_m is the elevation angle of the mask which related to the satellite azimuth angle φ_m, h is the relative height between the surrounding buildings and the UAV, and d is the distance between them.

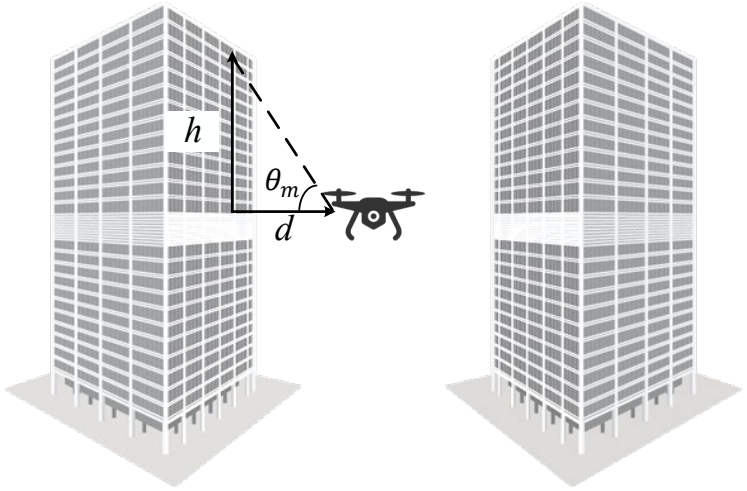

Figure 5 One UAV in the urban canyon scenario

Due to the finite width of the surrounding buildings, gaps are regarded necessary in the elevation mask. Figure 6 shows the satellite sky plot when applying an elevation mask. Two red lines delineate the silhouette of nearby buildings. The red dots stand for satellites from BDS, and the blue ones for satellites from GPS. The grey dots represent the satellites that are blocked by buildings. For vehicles not influenced by GNSS blockage, the maximum number of available satellites equals to 10.

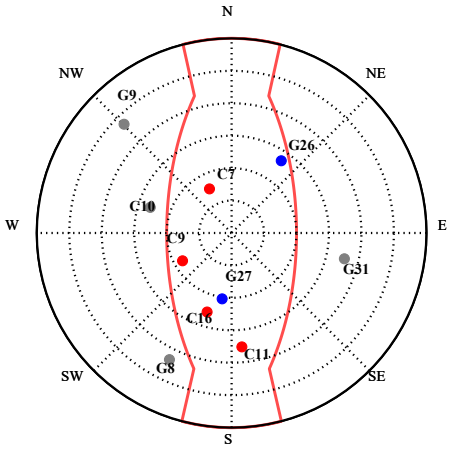

Figure 6 Satellite sky plot for a UAV in urban environment when $h/d = \sqrt{3}$

Unless otherwise specified, the proposed cooperative navigation approach is applied based on double differenced transfer method.

4.2 Results

The simulation results focus on the positioning performance of the UAV in the urban environments.

As shown in Figure 7, simulation results manifest that the positioning error in all three directions plummets when applying cooperative navigation based on virtual centroid. It is worth noting that the UAV encountered severe GNSS signal blockage occasionally and thus failed to locate itself. The positioning error in certain periods was manually set to [16, 16, 16] m in ENU coordinates, which was circled in yellow. The cooperative navigation method proposed in this paper helps to avoid losing position estimates in harsh GNSS signal environments. To better evaluate the positioning performance, the epochs with failure to locate are omitted in the following analyses.

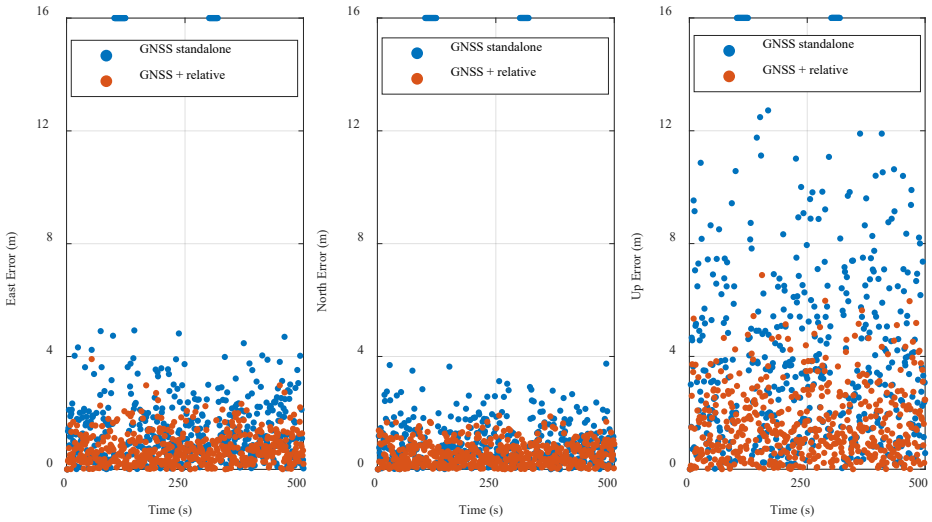

Figure 7 Positioning error of UAV in urban settings

Figure 8 compares the performance of two navigation approaches when applied in GNSS degraded environments in terms of cumulative distribution functions. As shown in this set of figures, at the same level of positioning error, cooperative navigation gains a higher cumulative probability than standalone GNSS navigation, which shows an evidence of preferred positioning accuracy. For example, with SDT method, this approach managed to provide a 3 m positioning accuracy with 78% probability against 37% for standalone GNSS scheme. The comparison between Figure 8 (a) and (b) shows no distinct difference on positioning accuracy between two transfer methods.

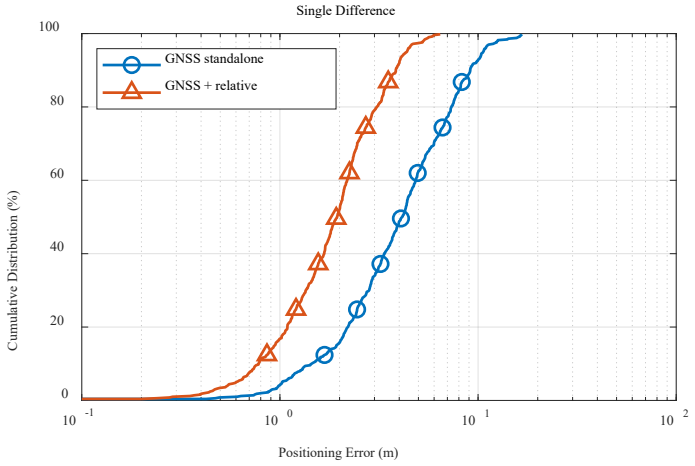

(a)

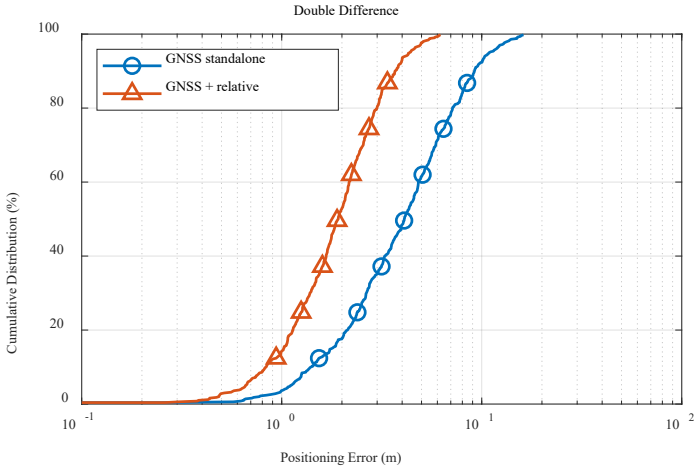

(b)

Figure 8 Cumulative distribution for UAV in urban settings

The positioning error is evaluated by means of square of covariance (labeled as SIG) and standard deviation (labeled as STD). SIG demonstrates the standard deviation of positioning error without a loss of generality. Judging from Figure 9, the numerical analysis on covariance is proofed effective due to negligible difference between SIG and statistical STD for both navigation methods.

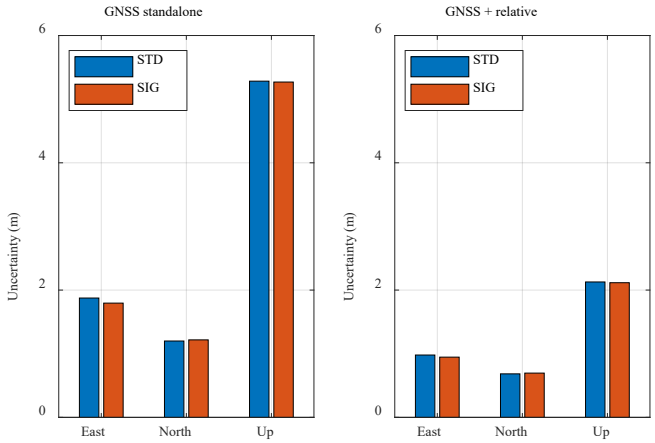

Figure 9 STD and SIG of the positioning error for UAV in urban settings

The numerical results are noted in Table 1 which compares the precision of positioning solution of standalone GNSS navigation and cooperative navigation. The purpose of developing covariance matrix is to estimate the positioning error and thus perform sensitivity analyses on the premise of knowing the external environment, i.e. satellite elevation angle, the number of satellites and relative measurement accuracy.

Table 1 Statistical Analysis of the Precision of Two Positioning Approaches for the UAV in Urban Environments

Scheme		Mean [m]	STD [m]	SIG [m]
E	GNSS standalone	1.441	1.875	1.795
	GNSS + relative	0.764	0.980	0.946
N	GNSS standalone	0.949	1.200	1.218
	GNSS + relative	0.531	0.684	0.696
U	GNSS standalone	4.054	5.283	5.269
	GNSS + relative	1.700	2.128	2.116

The improvement of the positioning results when applying cooperative scheme depends on the surrounding environments. Considering that absolute measurements are prone to signal blockage and multipath whereas relative measurements are robust enough, it is necessary to study the effects of environmental factors.

As shown in Figure 10, the improvement achieved declines with the increase of the number of visible satellites. The cooperative navigation algorithm is particularly effective on improving accuracy when the UAV has limited access to satellite signals. The proposed algorithm aims to mitigate the effect of multipath and receiver noise on positioning accuracy. This figure suggests that compared to the undifferential case, the improvement is more significant when applying differential corrections. This is because the common error imposed by ephemeris and troposphere is eliminated, which leaves multipath as the dominant factor of positioning error.

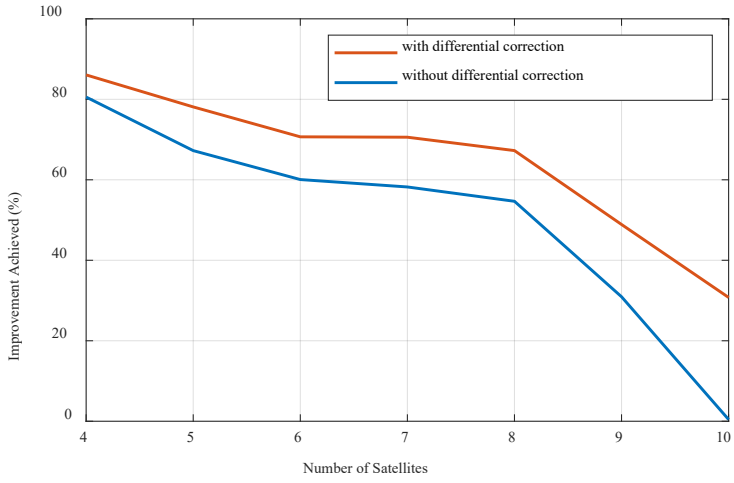

Figure 10 Improvement achieved according to the number of LOS satellites

Figure 11 describes the positioning error effected by the number of LOS satellites. The positioning error of standalone GNSS navigation drops when an increase is seen on the number of LOS satellites, which explains the decrement of positioning accuracy gains as cooperative navigation always keeps the positioning accuracy at a constant level. It is worth noting that, in standalone GNSS navigation, the minimum requirements for the number of visible satellites equals to 4. However, only when the 4 satellites belong to the same constellation is the UAV capable of calculating its absolute position. Satellites from another constellation bring clock bias as an unknown

variable in the process of positioning. As in Figure 11, standalone GNSS navigation as well as SDT cooperative navigation cannot be performed when the number of LOS satellites is less than 4, whereas DDT cooperative navigation eases the restriction to 1 visible satellite in Figure 11 (c) and (d).

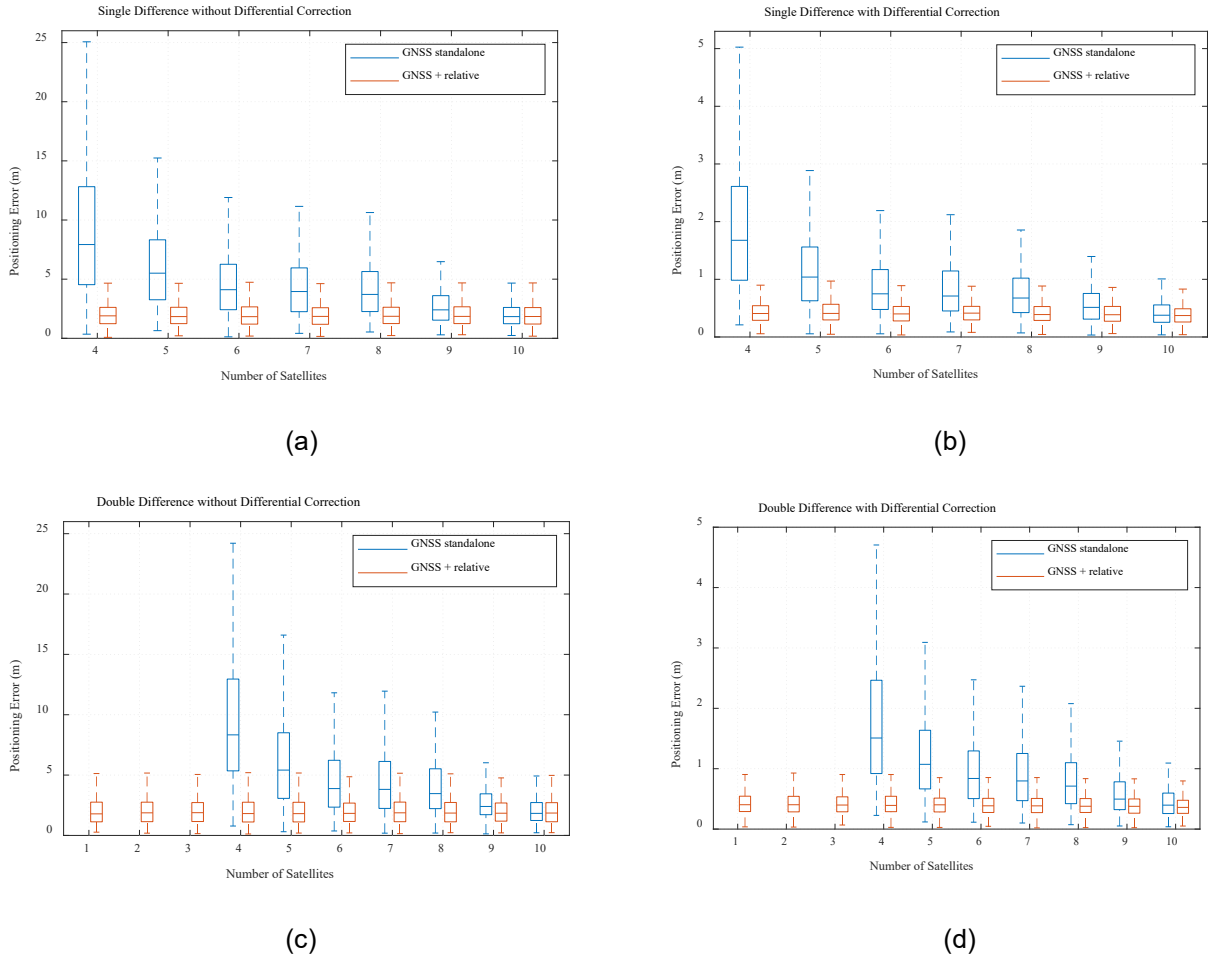

Figure 11 Positioning error in terms of the number of LOS satellites

Table 2 compares the gain of positioning accuracy with respect to the scale of UAV swarm with and without differential correction. It is clear that the cooperative scheme achieves better performance when applied in large-scale swarm. Additionally, differential correction is considered as an available means to achieve better positioning performance owing to the development of base stations.

Table 2 Improvement Achieved Considering Different Scales of UAV Operations

	Number of UAVs	2	5	10	20	50
Improvement achieved	without differential correction	56.21%	57.53%	57.92%	58.11%	58.23%
	with differential correction	33.18%	59.07%	71.27%	79.76%	87.22%

Besides the cooperative navigation method proposed in this paper, another cooperative approach is also evaluated. The common approach of cooperative navigation aims to acquire the absolute position of a master first and then broadcast its position to slaves which calculate their positions based on relative measurements instead of their own GNSS observations. The master here can be regarded as an anchor node. In the traditional cooperative approach, the slaves cast aside their GNSS observations and fully rely on the positioning result from the master, while the observations are fully used in our

approach. The increase of observations mitigates receiver noise and multipath.

With regard to fluctuating accuracy of relative measurements, the improvement of cooperative navigation varies. Figure 12 demonstrates that the gains of positioning accuracy creep down with the increase of relative positioning error. More specifically, Figure 12 (a) displays the improvement achieved in the application of cooperative navigation methods without differential correction, whereas Figure 12 (b) shows the results with differential correction.

Compared to the blue line, the red line in the same plot lies above it all the time, which shows the robustness of our approach even when the UAVs are equipped with low-cost sensors. Notice that in Figure 12 (b) traditional cooperative navigation method provides no improvement when the relative positioning error is larger than [0.5, 0.5, 0.5] m in ENU coordinates. The underlying causes originate from the slaves' discarding their GNSS observations. They are so dependent on relative navigation that once the master fails to provide high-accuracy location, or the accuracy of relative measurements are degraded, the slaves using this traditional cooperative navigation method run the risk of getting worse results than operating standalone GNSS navigation.

The comparison between Figure 12 (a) and (b) displays a significant difference of performance enhanced. It should be noted that the approach proposed in this paper makes full use of all GNSS observations, whereas only those from the master are utilized in traditional cooperative approach. Redundant information helps to reduce the error caused by receiver related thermal noise and multipath. In this regard, the cooperative navigation method based on virtual centroid is superior to the traditional one.

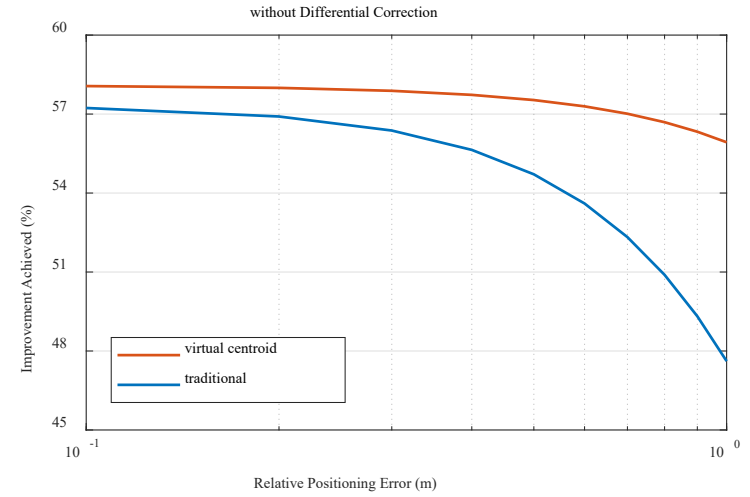

(a)

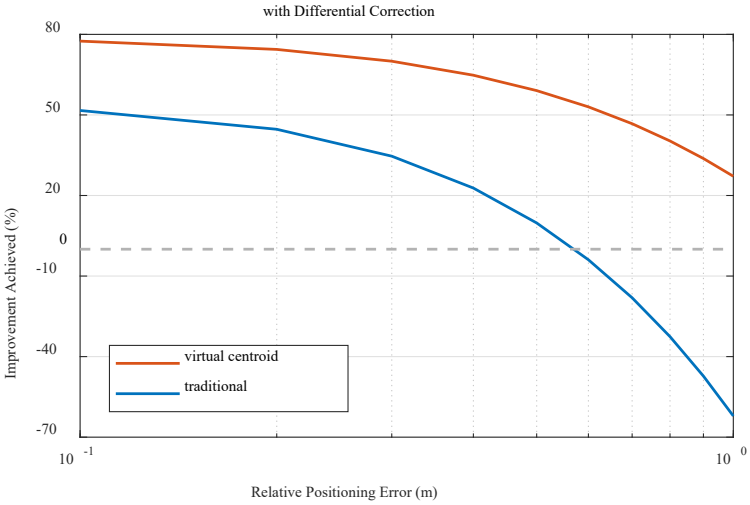

(b)

Figure 12 Gain of positioning accuracy affected by relative error

IV. CONCLUSION

This paper proposed a cooperative navigation approach to ensure high accuracy of absolute positioning for UAV swarms by utilizing easily accessible relative measurements and GNSS observations from neighboring UAVs. The approach is particularly suitable for urban environments. After a concise description of the relevant measurement formulas and the algorithm we propose, the concept of covariance matrix was introduced and applied to sensitivity analysis. Covariance matrix takes the error from GNSS observations and relative measurements into account and displays the uncertainty level of positioning. Simulation results revealed that in GNSS-challenging environments, the proposed approach outperformed standalone GNSS navigation by achieving a 59.07% or 57.53% improvement of positioning error with or without differential correction. The approach proposed in this paper managed to provide a 3 m position accuracy with 78% probability against 37% for standalone GNSS scheme. In comparison with traditional cooperative navigation approach, our approach was proved more robust even when the UAVs were equipped with low-cost relative sensors. For our future work, we will focus on flight testing to validate and analyze the performance of our approach.

APPENDIX

A. Proof of Covariance Matrix for the Error of Equivalent GNSS Observations

The covariance term for two equivalent GNSS observations is expressed as

$$\begin{aligned}\operatorname{cov}\left(\tilde{\rho}_p^{*j},\tilde{\rho}_q^{*k}\right) &= \operatorname{cov}\left(\tilde{\rho}_p^{j}+\tilde{\rho}_{pc}^{j},\tilde{\rho}_q^{k}+\tilde{\rho}_{qc}^{k}\right)\\ &= \operatorname{cov}\left(\tilde{\rho}_p^{j}+\tilde{d}_{pc}^{j},\tilde{\rho}_q^{k}+\tilde{d}_{qc}^{k}\right)\\ &= \operatorname{cov}\left(\tilde{\rho}_p^{j},\tilde{\rho}_q^{k}\right)+\operatorname{cov}\left(\tilde{d}_{pc}^{j},\tilde{d}_{qc}^{k}\right)\end{aligned} \tag{A.1}$$

where c represents virtual centroid.

There are four cases when dealing with the covariance:

(1) $j=k$ & $p=q$. In this case, the covariance is identical to variance.

$$\begin{aligned}\operatorname{cov}\left(\tilde{\rho}_p^{*j},\tilde{\rho}_q^{*k}\right) &= \sigma^2\left(\tilde{\rho}_p^{j}\right)+\sigma^2\left(\tilde{d}_{pc}^{j}\right)\\ &= \sigma^2\left(\tilde{\rho}_p^{j}\right)+\sigma^2\left(\mathbf{1}^{j}\cdot\tilde{\boldsymbol{x}}_{pc}\right)\\ &= \sigma_{URE,j}^2+\sigma_{tropo,j}^2+\sigma_{user,j}^2\\ &\quad+\mathbf{1}^{j}\cdot\boldsymbol{C}_d\cdot\left(\mathbf{1}^{j}\right)^{\mathrm{T}}\\ &= \sigma_{URE,j}^2+\sigma_{tropo,j}^2+\sigma_{user,j}^2+\sigma_d^2\end{aligned} \tag{A.2}$$

(2) $j=k$ & $p\neq q$, which means the two observations that are generated from different receivers aim at the same satellite. Since the relative measurement error is irrelevant for two receivers, $\sigma^2\left(\tilde{d}_{pc}^{j}\right)=0$. Similarly, the error related to multipath and receiver thermal noise is not considered.

$$\begin{aligned}\operatorname{cov}\left(\tilde{\rho}_p^{*j},\tilde{\rho}_q^{*k}\right) &= \sigma^2\left(\tilde{\rho}_p^{j}\right)\\ &= \sigma_{URE,j}^2+\sigma_{tropo,j}^2\end{aligned} \tag{A.3}$$

(3) $j\neq k$ & $p=q$. The observations originate from one single UAV and serve for satellite j and k individually, therefore the error elements that come from absolute measurements are independent and contribute zero to the covariance.

$$\begin{aligned}\operatorname{cov}\left(\tilde{\rho}_p^{*j},\tilde{\rho}_q^{*k}\right) &= \sigma^2\left(\tilde{d}_{pc}^{j}\right)\\ &= \mathbf{1}^{j}\cdot\boldsymbol{C}_d\cdot\left(\mathbf{1}^{k}\right)^{\mathrm{T}}\\ &= \sigma_d^2\cdot\cos\left(\theta_{jk}\right)\end{aligned} \tag{A.4}$$

(4) $j\neq k$ & $p\neq q$. The two equivalent GNSS observations are completely independent.

$$\operatorname{cov}\left(\tilde{\rho}_p^{*j},\tilde{\rho}_q^{*k}\right)=0 \tag{A.5}$$

B. Proof of Covariance Matrix of Positioning Error

The covariance matrix of positioning error at virtual centroid is expressed as $\boldsymbol{H}^*$. Linearizing the covariance matrix for the positioning error of UAV q yields

$$\begin{aligned}\boldsymbol{H}_q &= \sigma^2\left(\tilde{\boldsymbol{p}}_q\right)\\ &= \sigma^2\left(\tilde{\boldsymbol{p}}^{*}+\tilde{\boldsymbol{x}}_{pc}\right)\\ &= \sigma^2\left(\tilde{\boldsymbol{p}}^{*}\right)+\sigma^2\left(\tilde{\boldsymbol{x}}_{qc}\right)+2\cdot\operatorname{cov}\left(\tilde{\boldsymbol{p}}^{*},\tilde{\boldsymbol{x}}_{qc}\right)\\ &= \boldsymbol{H}^{*}+\boldsymbol{C}_d+2\cdot\operatorname{cov}\left(\boldsymbol{S}\cdot\left(\boldsymbol{E}_q\cdot\tilde{\boldsymbol{x}}_{qc}\right),\tilde{\boldsymbol{x}}_{qc}\right)\\ &= \boldsymbol{H}^{*}+\boldsymbol{C}_d+2\cdot\boldsymbol{S}\cdot\boldsymbol{E}_q\cdot\boldsymbol{C}_d\end{aligned} \tag{B.1}$$

where:

$\tilde{\boldsymbol{\rho}}$ is the m-by-1 vector composed of the errors of all raw pseudorange measurements;

$\tilde{\boldsymbol{p}}^{*}$ involves likewise m errors of corresponding equivalent GNSS measurements.

ACKNOWLEDGMENTS

This work was supported by Shanghai Jiao Tong University-University of Toronto Global Strategic Partnership Fund (2019 SJTU-UoT). The authors would also like to thank Jiawen Shen and Cheng Chi from School of Aeronautics and Astronautics, SJTU, for their technical supports.

REFERENCES

[1] Schmuck P, Chli M, "Multi-UAV collaborative monocular SLAM," in 2017 IEEE International Conference on Robotics and Automation (ICRA), 2017, pp. 3863–3870.

[2] Lee BH, Morrison JR, Sharma R, "Multi-UAV control testbed for persistent UAV presence: ROS GPS waypoint tracking package and centralized task allocation capability," in 2017 International Conference on Unmanned Aircraft Systems (ICUAS), 2017, pp. 1742–1750.

[3] Xie P, Petovello MG, "Measuring GNSS Multipath Distributions in Urban Canyon Environments," *IEEE Transactions on Instrumentation and Measurement*, Vol. 64, No. 2, 2015, pp. 366–377.
[4] Hansen JM, Johansen TA, Sokolova N, Fossen TI, "Nonlinear Observer for Tightly Coupled Integrated Inertial Navigation Aided by RTK-GNSS Measurements," *IEEE Transactions on Control Systems Technology*, Vol. 27, No. 3, 2019, pp. 1084–1099.
[5] Li RB, Liu JY, Zhang L, Hang YJ, "LIDAR/MEMS IMU integrated navigation (SLAM) method for a small UAV in indoor environments," in 2014 DGON Inertial Sensors and Systems (ISS), 2014, pp. 1-15.
[6] Shen F, Cheong JW, Dempster AG, "A DSRC Doppler/IMU/GNSS Tightly-coupled Cooperative Positioning Method for Relative Positioning in VANETs," *Journal of Navigation*, Vol. 70, No. 1, 2017, pp. 120-136.
[7] Gross JN, Gu Y, Rhudy MB, "Robust UAV Relative Navigation with DGPS, INS, and Peer-to-Peer Radio Ranging," *IEEE Transactions on Automation Science and Engineering*, Vol. 12, No. 3, 2015, pp. 935-944.
[8] Nguyen T, Qiu Z, Nguyen TH, Cao M, Xie L, "Distance-Based Cooperative Relative Localization for Leader-Following Control of MAVs," *IEEE Robotics and Automation Letters*, Vol. 4, No. 4, 2019, pp. 3641-3648.
[9] Qu Y, Wu J, Xiao B, and Yuan D, "A Fault-Tolerant Cooperative Positioning Approach for Multiple UAVs," *IEEE Access*, Vol. 5, 2017, pp. 15630-15640.
[10] Vetrella AR, Fasano G, Accardo D, Moccia A, "Differential GNSS and Vision-Based Tracking to Improve Navigation Performance in Cooperative Multi-UAV Systems," *Sensors (Switzerland)*, Vol. 16, No. 12, 2016, p. 2164.
[11] Sivaneri VO, Gross JN, "Flight-testing of a cooperative UGV-to-UAV strategy for improved positioning in challenging GNSS environments," *Aerospace Science and Technology*, Vol. 82-83, 2018, pp. 575-582.
[12] Sivaneri VO, Gross JN, "UGV-to-UAV cooperative ranging for robust navigation in GNSS-challenged environments," *Aerospace Science and Technology*, Vol. 71, 2017, pp. 245-255.
[13] Ko H, Kim B, Kong S, "GNSS Multipath-Resistant Cooperative Navigation in Urban Vehicular Networks," *IEEE Transactions on Vehicular Technology*, Vol. 64, No. 12, 2015, pp. 5450-5463.
[14] Wang SZ, Zhan XQ, Zhai YW, Chi C, Shen JW, "Highly reliable relative navigation for multi-UAV formation flight in urban environments," Chinese Journal of Aeronautics, 2020.
[15] Hoang GM, Denis B, Härri J, Slock DTM, "Cooperative localization in GNSS-aided VANETs with accurate IR-UWB range measurements," in 2016 13th Workshop on Positioning, Navigation and Communications (WPNC), 2016, pp. 1-6.
[16] Liu J, Cai BG, Wang J, "Cooperative Localization of Connected Vehicles: Integrating GNSS With DSRC Using a Robust Cubature Kalman Filter," *IEEE Transactions on Intelligent Transportation Systems*, Vol. 18, No. 8, 2017, pp. 2111-2125.
[17] Martinelli A, Pont F, Siegwart R, "Multi-Robot Localization Using Relative Observations," in Proceedings of the 2005 IEEE International Conference on Robotics and Automation, 2005, pp. 2797-2802.
[18] Si SB, Zhang YG, Luo L, Li N, "A New Underwater All Source Positioning and Navigation(ASPN) Algorithm Based on Factor Graph," in 2019 Chinese Control And Decision Conference (CCDC), 2019, pp. 2742-2746.
[19] Teunissen P, Montenbruck O, Springer handbook of global navigation satellite systems. Springer, 2017.
[20] Blanch J, Walker T, Enge P, Lee Y, Pervan B, Rippl M, Spletter A, Kropp V, "Baseline advanced RAIM user algorithm and possible improvements," *IEEE Transactions on Aerospace and Electronic Systems*, Vol. 51, No. 1, 2015, pp. 713-732.
[21] Sorenson HW, "Least-squares estimation: from Gauss to Kalman," *IEEE Spectrum*, Vol. 7, No. 7, 1970, pp. 63-68.
[22] del Peral-Rosado JA, Saloranta J, Destino G, López-Salcedo JA, Seco-Granados G, "Methodology for simulating 5G and GNSS high-accuracy positioning," *Sensors (Switzerland)*, Vol. 18, No. 10, 2018, p. 3220.